On the Feasibility of Network RF Energy Operated Field Sensors

Swades De[a], Aditya Kawatra[b], and Shouri Chatterjee[c]

[a,c]Electrical Eng. Dept., Indian Institute of Technology Delhi, New Delhi, India

[b]Ecole Polytechnique, Palaiseau, France

Abstract— This paper estimates the feasibility of operating field sensors using otherwise unwanted radio frequency (RF) energy in a wireless ad hoc sensor network. In the traditional concept, an exposed node is kept from any communication activities during a neighbor's transmission. To save energy, the node may go to sleep mode during its inactivity period. In contrast, it is proposed that whenever a node is not communicating it should attempt to collect energy from the ongoing transmissions in its vicinity.

A two-tier network is considered with the field sensor nodes having rudimentary communication (transmission) functionality at the first tier and the routing-capable nodes at the second tier. Via geometric probabilistic analysis, aided by network simulations, the conditions on rectification efficiency and transmission duty cycle of network RF energy operated field nodes are derived for their uninterrupted processing and transmission activities.

I. INTRODUCTION

There have been significant ongoing efforts on how to impart energy to the depleted batteries of wireless nodes on-line. Prior on-line battery recharging sources include vibrations [1], wind energy [2], water current [3], thermal gradient and strain from human activities [4], ambient (other than in-network) radio frequency (RF) energy [5], solar energy [6], etc., as well as a combination of them [7]. Wireless recharging from high power RF source has also been demonstrated recently [8].

As an alternative, here we aim at evaluating the possibility of on-line recharging of wireless nodes from in-network RF energy, as it does not require any dedicated energy source. Note that, as long as an otherwise idling sensor node is capable of gleaning energy from the RF waves and the rectification efficiency is sufficiently high that ensures the charging rate is at least equal to the energy dissipation rate (during transmission and other nodal processing activities), one would in principle have perpetually powered wireless sensor nodes.

Our contribution in this paper are: (a) Via geometric probabilistic analysis, verified by network simulations, we obtain the power available at a field node that is exposed to transmissions from possibly more than one surrounding router nodes. (b) Via numerical calculations using practical parameter values we show that, by suitably adjusting the sleep cycle length, a field sensor can perpetually run by the in-network RF energy. For example, our calculations show that, with 5% rectification efficiency, the activities of field sensors, operating at 915 MHz, can be sustained with network RF energy by transmitting 40 Bytes long data frames with 27 minutes duty cycle.

In Section II, network architecture and channel access properties are outlined. The analysis of available RF power at the field nodes is presented in Section III. Key numerical and simulation results on available power are discussed in Section IV. Current state-of-the-technology on low power sensors is surveyed in Section V. In Section VI, the field nodes' possible activity duty cycle in relation to energy rectification efficiency is evaluated. The paper is concluded in Section VII.

II. NETWORK ARCHITECTURE AND ACCESS FRAMEWORK

A. Nodal architecture and activity pattern

Each field node is assumed equipped with a rectifying circuit along with its rechargeable battery. In conventional CSMA (carrier-sense multiple access), when a neighboring transmission is detected, to save energy, a node would go to sleep mode during a pre-decided back-off duration. Or, if the communication activity of the nodes are sporadic, a node would remain in sleep state unless it has something to transmit. In contrast to the traditional approaches, we propose that whenever a node is not communicating, it should attempt to collect energy from the ongoing neighboring transmissions by directing the received signal power to the recharging unit.

Since communication related activities consume most of the energy, to gain from network energy scavenging a node should communicate sporadically and have very little leakage current.

B. Network architecture

We consider a two-tier network architecture, where the energy constrained field nodes with rudimentary communication functionality are placed in tier-1 (lower tier), and the routing-capable nodes are placed in tier-2 (higher tier). The field nodes are star connected with the router nodes. A field node remains sporadically active and wirelessly transmits (without expecting an acknowledgment) its sensed data to a router with which it is attached. During its processor inactivity period it attempts to replenish its battery from the RF energy which comes from the router nodes' (also, in principle, from other field nodes') transmission activities. Due to the uncoordinated activity of field nodes, some data loss is expected. In this work, however, instead of dealing with the data loss, we will evaluate the feasibility of powering the field nodes from in-network energy.

A tier-2 router node has full-fledged communication capabilities and it can communicate with any one of the nearby tier-2 nodes to transfer the collected data toward a sink. They form a multi-hop ad hoc network among themselves, and are assumed to be active most of the time in accumulating and forwarding data and contending for channel access. In

this work we will assume that they have uninterrupted power supply. In practice uninterrupted tier-2 network operation can be achieved by either introducing nodal mobility (replacing the energy depleted nodes and reconfiguring the network connectivity) or having some kind of recharge capability from other natural energy sources, such as photovoltaic energy.

III. ANALYSIS OF AVAILABLE POWER FOR SCAVENGING

We analyze the available RF power at a tier-1 node in presence of tier-2 nodes' ad hoc communication activities, where a system steady state is assumed. Transmission activity of a tier-1 node being very sporadic, it can be shown that the power available from other tier-1 nodes' transmissions is negligible compared to that from the tier-2 nodes. Let us first distinguish between a *receiver* and a *scavenger* node.

Definition 1: A node that extracts information from the received RF wave is termed as a receiver. A node that extracts energy without being aware of the signal content in the RF wave is termed as a scavenger.

In context of our discussion, only a tier-2 node can be a receiver and a tier-1 node can be a scavenger.

A. Considerations and assumptions on network properties

1) The nodes are distributed as a two-dimensional spatial Poisson point process with density ρ. That is, the probability of finding i nodes in an area of size A is

$$p(i) = \frac{(\rho A)^i}{i!} e^{-\rho A}. \tag{1}$$

2) The channel access protocol is slotted CSMA/CA (CSMA with collision avoidance) without RTS/CTS (request-to-send and clear-to-send) signals.

3) Tier-2 nodes have circular communication coverage with radius R_T and CS radius R_C. Typically, $R_C \approx 2R_T$.

4) A transmitter's one-hop receiver can be located anywhere within its communication range R_T.

5) Transmission attempt rate or the probability of a transmission attempt in a slot p_{tr} is the same at all nodes.

6) Tier-1 nodes have circular transmission range of radius R_F, where $R_F \approx \frac{R_T}{2}$. For simplicity, CS range of tier-1 nodes is taken same as that of tier-2 nodes.

7) The power available at a tier-1 node depends on polynomial decay of signal strength with distance, where the time variability due to channel fading is discounted.

B. Some observations

Lemma 1: In a network with homogeneous communication coverage and CSMA/CA based channel access, the maximum number of simultaneously transmitting tier-2 nodes in the CS range of a tier-1 node is limited to 5.

Proof: In Fig. 1, the distance d_s of the tier-1 node S from X is $0 < d_s \leq R_F$. During the transmission from X, by CSMA principle the nodes in its CS zone are kept from transmitting. However, since S is equally sensitive as a normal receiver (assumption 6), the additional energy available at S is from the nodes in its CS zone of radius R_C but outside that of X
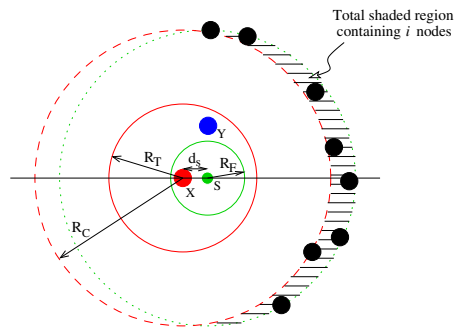

Fig. 1.   The scavenging concept.

(the shaded zone in Fig. 1). Due to CSMA, out of these nodes the ones that are away from each other by at least a distance R_C are allowed to simultaneously transmit. For a given d_s this number is maximum when the transmitting nodes in the shaded zone are on its outer rim. Hence, including the node X, the maximum total number of simultaneously transmitting nodes n_t around S can be found as:

$$n_t = \left\lfloor \frac{2\left(\pi - \arccos\frac{d_s}{2R_C}\right)}{\pi/3} \right\rfloor + 2. \tag{2}$$

From (2), n_t is maximum when $d_s = R_F \approx \frac{R_C}{4}$, and the maximum value is 5. ∎

C. Power availability analysis

The expression for the available power at a tier-1 node is obtained via geometric probabilistic calculations.

By assumption 7, the RF power at a distance d from a transmitter can be expressed as:

$$P_r(d) = \frac{P_t(\text{eff})}{d^\gamma}, \tag{3}$$

where $P_t(\text{eff}) = \frac{P_t d_0^\gamma}{\text{PL}[d_0]}$, P_t is the signal transmission power, γ is the path loss exponent, d_0 is the reference distance, and $\text{PL}[d_0]$ is the fixed loss up to d_0.

To find the total network RF power at a tier-1 node we first find the conditional average power available at S, $P_{s|X}(d_s)$, given that the transmitter X is 'on' at a distance d_s from S.

By (3), the power contribution of X to S $P_0(d_s)$ is: $P_0(d_s) = \frac{P_t(\text{eff})}{d_s^\gamma}$. Referring to Fig. 1, out of i ($i > 0$) nodes (with probability $p(i)$ given by (1)) in the shaded region of area A, by Lemma 1, there could be up to 4 additional simultaneously transmitting nodes. Denote by $P_{ij}(A)$ the average power available at S from only j transmitters ($j \leq \min\{i,4\}$) out of total i nodes in the shaded region of area A (a function of d_s), given that there are i nodes in the region. The total conditional average power available at S is given by:

$$P_{s|X}(d_s) = P_0(d_s) + \sum_{i=1}^{\infty} \sum_{j=1}^{\min\{i,4\}} p(i) P_{ij}(A)$$

$$= P_0(d_s) + \sum_{j=1}^{4} P_j(d_s), \tag{4}$$

where $P_j(d_s) = \sum_{i=j}^{\infty} p(i)P_{ij}(A)$, for $1 \le j \le 4$, is the contribution of j effective transmitters from the area A.

To calculate P_1, we refer to Fig. 2 showing an example case of $i = 3$ nodes in the total shaded region. Let, N_1 is
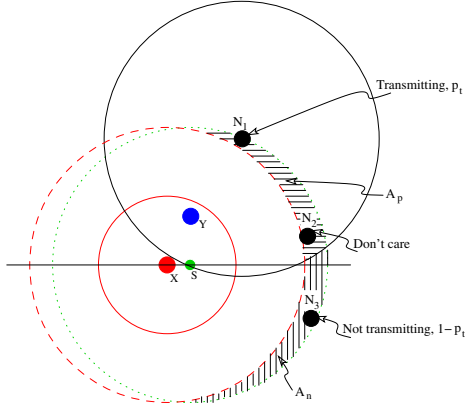

Fig. 2. An example scenario that contributes to P_{31}.

transmitting (with probability p_{tr}) in the same slot along with X. The horizontally shaded region is covered by N_1's CS zone. Since N_2 is located inside N_1's CS zone, it cannot initiate a transmission in the same slot. N_3 on the other hand is located outside the CS range of N_1, and so it could potentially be another simultaneous transmitter. Let, N_3 is not transmitting (with probability $1 - p_{tr}$) in the same slot with X and N_1. This setting corresponds to the power contribution $P_{31}(A)$.

Let N_1 be located at (r, θ) within a strip of infinitesimal area $dA = r \cdot dr \cdot d\theta$. Referring to Fig. 2, the probability that there are i_1 (respectively, i_2) additional nodes in the area A_p (respectively, A_n) (excluding the infinitesimal area dA) is:

$$\frac{(\rho A_p)^{i_1}}{(i_1)!} e^{-\rho A_p} \triangleq p(r, \theta)_{i_1}, \text{ and } \frac{(\rho A_n)^{i_2}}{(i_2)!} e^{-\rho A_n} \triangleq p(r, \theta)_{i_2}^{(c)}. \tag{5}$$

Using the notations in (5) with i_1 and i_2 replaced by 0, the available power at S from one-out-of-one node in the total shaded area, $P_{11}(d_s)$, is given by:

$$P_{11}(A) = \int_\theta \int_r p(r, \theta)_0 \cdot p(r, \theta)_0^{(c)} \cdot p_{tr} \frac{P_t(\text{eff})}{r^\gamma} \rho r dr d\theta.$$

To obtain $P_{21}(A)$, note that there could be two scenarios: first, both nodes are located in the area A_p and only one transmits (with probability p_{tr}); second, the transmitting node is in the area A_p and the non-transmitting node (with probability $1 - p_{tr}$) is in A_n. In general, the expression for P_{i1} is:

$$P_{i1}(A) = \frac{1}{i} \sum_{k=0}^{i-1} \int_\theta \int_r p(r, \theta)_k \cdot p(r, \theta)_{i-k-1}^{(c)}$$
$$\cdot p_{tr}(1 - p_{tr})^{i-k-1} \frac{P_t(\text{eff})}{r^\gamma} \rho r dr d\theta. \tag{6}$$

We obtain $P_{i2}(A)$ recursively, as it requires P_{k1}, although it is now computed over the complement area A_n. The

expression for $P_{i2}(A)$ is obtained as:

$$P_{i2}(A) = \frac{1}{i} \sum_{k=0}^{i-2} \int_\theta \int_r p(r, \theta)_k \cdot p(r, \theta)_{i-k-1}^{(c)}$$
$$\cdot p_{tr} \left[\frac{P_t(\text{eff})}{r^\gamma} + P_{i-k-1,1}(A_n) \right] \rho r dr d\theta. \tag{7}$$

Extending the approach in (7), the expression for the power available at S due to j out of i nodes in the shaded region is:

$$P_{ij}(A) = \frac{1}{i} \sum_{k=0}^{i-j} \int_\theta \int_r p(r, \theta)_k \cdot p(r, \theta)_{i-k-1}^{(c)}$$
$$\cdot p_{tr} \left[\frac{P_t(\text{eff})}{r^\gamma} + P_{i-k-1,j-1}(A_n) \right] \rho r dr d\theta, \tag{8}$$

for $i \ge j$ and $j \ge 2$. Here, by Lemma 1, j is limited to 4.

From the above, $P_j(d_s) = \sum_{i=j}^{\infty} p(i)P_{ij}(A)$ for $1 \le j \le 4$. The limits of r in the integrations are $R_C - d_s$ and R_C, and those of θ are functions of d_s and r.

IV. NUMERICAL AND SIMULATION RESULTS

We have obtained quantitative results on available power at a tier-1 node using (4) and by numerically solving (6) and (8). The effect of virtual carrier sensing via RTS/CTS handshake (when the tier-2 nodes are 802.11 based), i.e., the impact of X-Y distance in Fig. 2, has also been computed numerically. Key analytic results have been verified by simulating a random tier-2 network setting using C++, with CSMA/CA access method and without frame acknowledgments.

In numerical computation and simulations, the average number of neighborhood nodes $N = \rho \pi R_T^2$, X-Y distance d, X-S distance d_s, and transmission probability of a tier-2 node in a slot p_{tr} were kept variable. Operational frequency was taken 915 MHz. Reference distance was considered $d_0 = 2d_f$, where $d_f = \frac{2D^2 f}{c}$ is the Fraunhofer distance, D is the largest dimension of the antenna (considered 5 cm), and $c = 3 \times 10^8$ m/s is the speed of RF wave in air. For calculating path loss, we took antenna gains $G_r = G_t = 1$ (isotropic), system loss factor $L = 1$, and path loss exponent $\gamma = 2$. As per Texas Instrument's CC1100 data sheet [9], transmit power of tier-2 nodes was taken $P_t = 5$ dBm, at 915 MHz which gives about -53 dBm signal strength at 20 m distance from the transmitter, whereas the data-sheet specified saturation value of receive signal strength, when operating at 250 kBaud data rate, is -16 dBm. Accordingly, transmission radius of tier-2 nodes R_T was taken 20 m, and hence, $R_C = 40$ m.

Numerically computed plots in Fig. 3 shows the effect of RTS/CTS on the available power at a tier-1 node. Although with RTS/CTS it is expected to have a reduced number of simultaneously transmitting tier-2 nodes around a tier-1 node (which varies with X-Y distance), the plots show that there is almost no effect of a tier-2 receiver location on the available power at a tier-1 scavenger node. This is because, (referring to Fig. 1) distance of the transmitter X to the node S is smaller compared to the other potential tier-2 transmitters, and hence the power available at S is dominated by that from X. The
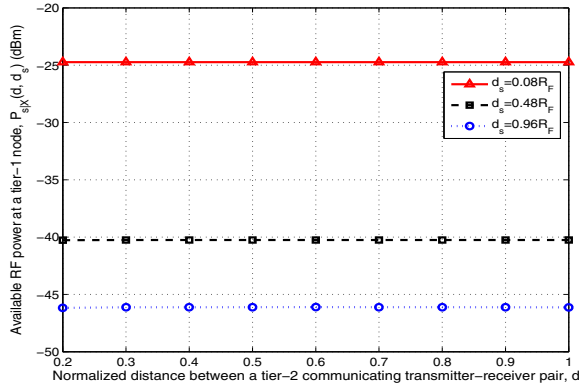
Fig. 3. Effect of X-Y distance (normalized with respect to R_T) on the available RF power at a tier-1 node. $N = 10$ and $p_{tr} = 0.3$.

plots thus reflect that the additional virtual carrier sensing, if employed at the tier-2 nodes, does not have a significant impact on the RF power availability at the tier-1 nodes.

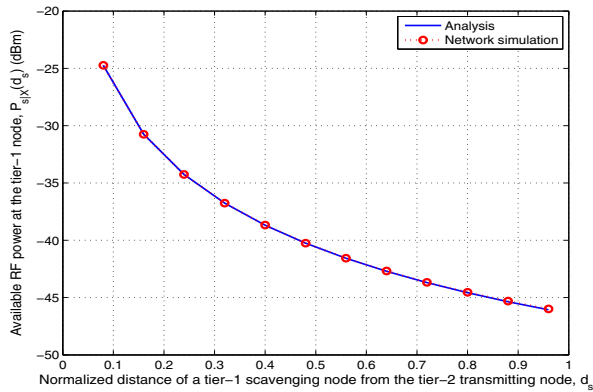Fig. 4 shows the variation of available power as a function of X-S distance. When the node S is closest to the active

Fig. 4. RF power availability as a function of distance from a tier-1 transmitter d_s (normalized with respect to R_F). $N = 10$, $p_{tr} = 0.3$.

transmitter X, the power available is maximum, because the distance of other potentially simultaneous tier-2 transmitters to S is always greater than d_s. The analytic and network simulations based results match quite well, particularly at a smaller d_s. The slight mismatch at higher values of d_s could be due to lesser granularity in numerical computation.

The effect of transmission probability of tier-2 nodes p_{tr} on available power at S is shown in Fig. 5. Although there is an increasing trend on the power availability at S as a function of p_{tr} (which is intuitive), the magnitude of increase is very little. This is because, irrespective of how many nodes want to simultaneously transmit, only a limited number can succeed. The plots also magnify the mismatch of analytic results with respect to the simulations. The analytically predicted value is seen increasingly lower than that obtained from simulation, which could be due to granularity error in numerical computation of nested integral equations in the analysis. This
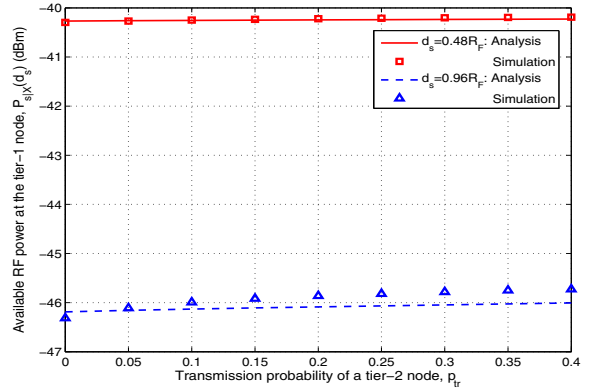

Fig. 5. Effect of p_{tr} on the available power at S. $N = 30$.

granularity introduces error by undermining the contribution of power from the neighboring transmitters (in the shaded zone of Fig. 1), which increases with the increase of d_s.

Below, we briefly survey the current state of technology on RF energy rectification and consumption requirements.

V. State of the Devices and Circuits Technology

On the RF energy rectification, broadband rectenna design studies in [5] showed that, with Schottky diode rectifiers, the conversion efficiency is only 0.1% at 5×10^{-5} mW/cm^2 incident power density (about -18 dBm, with 18.5 cm square antenna dimension). A CMOS rectifier based recharging circuit operating at 950 MHz [10] was demonstrated to operate at -14 dBm input power with a conversion efficiency of 1.2%. A further enhancement in [11] recently reported a rectification efficiency of up to 10% at -22.6 dBm input power.

On the consumption aspect, a miniature processor design for sensor network applications [12] shows that the CPU leakage consumption in the sleep mode is only about 30 pW and energy consumption per activity cycle is only 2.8 pJ. A system-on-chip design in [13] runs at about 1 V and consumes only a little above 2 mA current during transmit and receive modes. Combinedly, ultra-low power CPU and transceivers along with a reasonably high rectification efficiency can be exploited in our proposed network energy scavenging.

VI. Scavenged Network RF energy versus field nodes' activity pattern

In light of current state of the technology, here we evaluate the potential gain from network RF energy.

A. Energy requirement of tier-1 nodes

Consider that the the tier-1 nodes are equipped with 1 V RF transceivers [13]. To save energy, such a node is programmed to operate only in 'transmit' mode to send its sensed data to its tier-2 cluster-head once in a while. The transceiver operates at a voltage $V_{\text{on}} = 1.2$ V and draws a current $I_{\text{on}} = 2.635$ mA for an output transmit power -7 dBm. Thus, for a transmission of duration T_{on} seconds, the energy consumed by a tier-1 node would be: $E_{\text{on}} = V_{\text{on}} I_{\text{on}} T_{\text{on}} = 3.162 T_{\text{on}}$ mJ.

During rest of the time T_{sleep} s, the nodal processor remains in deep sleep mode, which could consume as low as $P_{\text{leak}} = 30$ pW [12]. The corresponding energy consumption would be: $E_{\text{leak}} = P_{\text{leak}} T_{\text{sleep}}$ pJ.

B. Condition of gain from network RF energy scavenging

To estimate the average scavenged power $P_s^{(\text{scv})}$, we have $P_{s|X}(d_s)$ from (4). Probability distribution function of d_s (uniform random variable) is: $\Pr[d_s] = \frac{2d_s}{R_F^2}$. With a tier-2 node's transmission probability p_{tr} and at a rectifier efficiency η, considering discrete data points, we have:

$$P_s^{(\text{scv})} = \eta p_{tr} \sum_{d_s = d_s^{(l)}}^{d_s^{(u)}} \Pr[d_s] P_{s|X}(d_s). \qquad (9)$$

Our calculation of network RF power is with the distance data set $d_s = \{0.08, 0.16, 0.24, 0.32, 0.4, 0.48, 0.56, 0.64, 0.72, 0.8, 0.88, 0.96\}$, normalized with respect to R_F. The scavenging gain is positive if $P_{\text{leak}} < P_s^{(\text{scv})}$. In the current network setting, with $P_{\text{leak}} = 30$ pW, and $p_{tr} = 0.3$ – for example, the positive gain occurs at about $\eta = 0.06\%$.

Additionally, the condition for network energy powered perpetual operation of sensor nodes is: $T_{\text{sleep}} = \frac{E_{\text{on}}}{P_s^{(\text{scv})} - P_{\text{leak}}}$.

To take a look into the effect of leakage power loss and scavenging circuit efficiency on the achievable transmission duty cycle of tier-1 nodes, we assume data frames are 40 Bytes long, and the transmission rate is 250 kbps, which gives $T_{\text{on}} = 1.28$ ms, hence $E_{\text{on}} = 4.0474$ μJ. Table I summarizes the performance at 915 MHz frequency, demonstrating the feasibility of running ultra power sensor nodes on scavenged network RF energy. The numerical figures in Table I show

TABLE I
Effect of scavenging efficiency η and leakage power P_{LEAK} on sleep duty cycle T_{SLEEP}. Tier-2 nodes' transmission probability $p_{tr} = 0.3$.

P_{leak} ($\eta = 1\%$)	T_{sleep}	η ($P_{\text{leak}} = 30$ pW)	T_{sleep}
0 pW	13.36 min	1%	142 min
30 pW	13.44 min	2%	69 min
1 nW	16.55 min	5%	27 min
10 nW	–	10%	13.44 min

that, with about 30% transmission activity at tier-2 router nodes, even at 10% rectification efficiency, the tier-1 field node operation using network RF energy is impossible if its sleep state consumption is more than a few nano-watts (as in current off-the-self sensors, such as CC1100 [9]). On the other hand, with 30 pW leakage power (as demonstrated in [12]), operation of field nodes using scavenged network RF energy becomes nearly infeasible below about 1% rectification efficiency. Overall, it appears that, with the available new technologies the leakage consumption of the processor is not the main bottleneck; rather rectification efficiency sets the operational limit of network energy operated field nodes.

VII. Conclusion

We have investigated the feasibility of network energy scavenging to reduce the battery life constraint in wireless sensor networks. Via probabilistic analysis we have shown that a field node can have only a limited amount of energy available from the nearby communicating nodes. We have further demonstrated that, thanks to the upcoming low power processors, for the field nodes with rudimentary communication capability, network energy scavenging gain can be positive even at a very low rectification efficiency. With a little improved rectification efficiency, the field nodes can even run fully on the network RF energy.

References

[1] S. Meninger, J. Mur-Miranda, R. Amirtharajah, A. Chandrakasan, , and J. Lang, "Vibration to electric energy conversion," *IEEE Trans. VLSI*, vol. 9, no. 1, pp. 64–76, Feb. 2001.

[2] M. Weimer, T. Paing, and R. Zane, "Remote area wind energy harvesting for low-power autonomous sensors," in *Proc. IEEE Electron. Specialists Conf.*, Jeju, South Korea, Jun. 2006, pp. 1–5.

[3] G. Taylor, J. Burns, S. Kammann, W. Powers, and T. Welsh, "The energy harvesting eel: A small subsurfaceocean/river power generator," *IEEE J. Oceanic Eng.*, vol. 26, no. 4, pp. 539–547, Oct. 2001.

[4] J. Gonzalez, A. Rubio, and F. Moll, "Human powered piezoelectric batteries to supply power of wereables electronic devices," *Int. J. Soc. Materials Eng. Resources*, vol. 10, no. 1, pp. 34–40, 2002.

[5] J. Hagerty, F. Helmbrecht, Q. McCalpin, R. Zane, and Z. Popovic, "Recycling ambient microwave energy with broad-band rectenna arrays," *IEEE Tran. Microwave Theory and Techniques*, vol. 52, no. 3, pp. 1014–1024, Mar. 2004.

[6] V. Raghunathan, A. Kansal, J. Hsu, J. Friedman, and M. Srivastava, "Design considerations for solar energy harvesting wireless embedded systems," in *Proc. Intl. Symp. Information processing in sensor networks*, Los Angeles, CA, USA, Apr. 2005.

[7] J. Paradiso and T. Starner, "Energy scavenging for mobile and wireless electronics," *IEEE Pervasive Computing*, pp. 18–27, Jan.-Mar. 2005.

[8] T. Paing, J. Morroni, A. Dolgov, J. Shin, J. Brannan, R. Zane, and Z. Popovic, "Wirelessly-powered wireless sensor platform," in *Proc. IEEE European Microwave Conf.*, Munich, Germany, Oct. 2007.

[9] "Texas Instrument CC1100 data sheet," 2009. [Online]. Available: http://focus.ti.com/lit/ds/symlink/cc1100.pdf

[10] T. Umeda, H. Yoshida, S. Sekine, Y. Fujita, T. Sujuki, and S. Otaka, "A 950 MHz rectifier circuit for sensor networktags with 10 m distance," *IEEE. J. Solid-State Circuits*, vol. 41, no. 1, pp. 35–41, Jan. 2006.

[11] T. Le, K. Mayaram, and T. Fiez, "Efficient far-field radio frequency energy harvesting for passively powered sensor networks," *IEEE J. Solid-State Circuits*, vol. 43, no. 5, pp. 1287–1302, May 2008.

[12] M. Seok, S. Hanson, Y.-S. Lin, Z. Foo, D. Kim, Y. Lee, N. Liu, D. Sylvester, and D. Blaauw, "The Phoenix processor: A 30pW platform for sensor applications," in *Proc. IEEE Symp. VLSI Citcuits*, Honolulu, HI, USA, June 2008, pp. 188–189.

[13] A. C. W. Wong, G. Kathiresan, C. K. T. Chan, O. Eljamaly, O. Omeni, D. McDonagh, A. J. Burdett, , and C. Toumazou, "A 1 V wireless transceiver for an ultra-low-powerSoC for biotelemetry applications," *IEEE J. Solid-State Circuits*, vol. 43, no. 7, pp. 1511–1521, July 2008.